Computation-guided redesign of promoter specificity of a bacterial RNA polymerase

Xiangyang Liu[1,‡], Anthony T. Meger[2,3,‡], Thomas Gillis[2,‡], and Srivatsan Raman[2,3,4,5,*]

[1]Biophysics Graduate Program, University of Wisconsin-Madison, Madison, Wisconsin 53706, United States

[2]Department of Biochemistry, University of Wisconsin-Madison, Madison, Wisconsin 53706, United States

[3]Great Lakes Bioenergy Research Center, University of Wisconsin-Madison, Madison, Wisconsin 53706, United States

[4]Department of Bacteriology, University of Wisconsin-Madison, Madison, Wisconsin 53706, United States

[5]Department of Chemical and Biological Engineering, University of Wisconsin-Madison, Madison, Wisconsin 53706, United States

[‡]These authors contributed equally to this work

Contact Information

*Corresponding author: Srivatsan Raman (sraman4@wisc.edu)

ABSTRACT

The ability to regulate circuits and pathways is central to cellular control. The existing toolkit is predominantly comprised of local transcription regulators that are unsuitable for exerting control at a global genome-wide scale. Bacterial sigma factors are ideal global regulators as they direct the RNA polymerase to thousands of transcription sites. Here, we redesigned the promoter specificity of the *E. coli* housekeeping sigma factor, sigma-70, toward five orthogonal promoter targets not recognized by the native sigma-70. These orthogonal sigma-70s were engineered by screening a pooled library of computationally-guided designs customized toward each promoter target. A combination of conserved interactions with the DNA backbone and target-specific interactions facilitate new promoter recognition. Activity of the top performing redesigned sigma-70s varied across the promoter targets and ranged from 17% to 77% of native sigma-70 on its canonical active promoter. These orthogonal sigma factors represent a new suite of regulators for global transcriptional control.

KEYWORDS: Protein-DNA interactions; Computational design; biological orthogonalization; specificity; high-throughput screening

36 **INTRODUCTION**

37 Synthetic biology aims to control cellular behavior through synthetic pathways and circuits. These pathways
38 and circuits depend on orthogonal gene regulation to selectively insulate them from host processes while
39 sharing central dogma resources and machinery with the host.[1-5] In bacteria, native gene regulation is
40 governed at the local and global levels.[6-8] At the local level, individual genes and operons are controlled by
41 transcription factors that are activated by specific metabolites or environmental cues. These local regulators
42 (i.e., small-molecule inducible transcription factors) have been co-opted and engineered to build a large
43 toolkit of orthogonal gene regulatory components for synthetic circuits and pathways.[9-12] At a global level,
44 the RNA polymerase (RNAP) is directed to hundreds to thousands of loci simultaneously by a battery of
45 sigma factors to maintain homeostasis and respond to environmental changes.[13] In contrast to local
46 regulators, efforts to engineer RNAP to exert control at a global level remain poorly developed. Although
47 some genes or operons can be regulated from synthetic promoters with non-native regulation, large
48 swathes of the bacterial genome, especially genes involved in core metabolic processes, require native
49 regulation as they are often layered in complex networks that cannot be easily disentangled.[3,14] Orthogonal
50 regulation in these genes can be introduced by modifying RNAP promoter specificities without disrupting
51 native regulation.[15] With emerging technologies to synthesize genomes from scratch, genome-scale
52 orthogonal gene regulation could be programmed into cells.[16,17] Such a system could have different RNAP
53 promoter specificities encoded in different regions of the genome to compartmentalize them. Thus,
54 redesigning the RNAP is a powerful but underexplored route to engineer orthogonal genetic regulation.
55
56 The sigma subunit of the bacterial RNAP governs the interaction of the RNAP with the promoter.[18-20] The
57 bacterial RNAP is a multi-subunit molecular machine composed of alpha, beta, omega, and sigma subunits.
58 The alpha, beta, and omega subunits form the core RNAP enzyme responsible for RNA synthesis using
59 DNA as a template and ribonucleotides as the substrate.[21,22] To initiate transcription, the core RNAP binds
60 to a sigma factor which directs the RNAP to specific promoters.[19,20,23,24] Bacteria express several types of
61 sigma factors that can recognize and bind specific promoters in response to cellular signals and
62 environmental conditions.[24-26] Of the seven types of sigma factors in *E. coli*, sigma-70 is the dominant as it
63 is responsible for expressing housekeeping genes, and the other sigma factors are only transiently

64 expressed during stress.[27-32] Prior strategies to engineer RNAP have used heterologous sigma factors from
65 other hosts or constructed chimeras of native and non-native sigma factors to engineer new RNAP promoter
66 specificities.[33-35] However, heterologous sigma factors are often toxic to the host, and chimeric sigma
67 factors are not orthogonal, limiting the extent to which they may be used in synthetic systems.[36,37]
68 Additionally, the use of heterologous and chimeric sigma factors is strain-dependent.[33] Despite the
69 attractiveness of the sigma factor as a target for orthogonal genetic regulation, we do not have well-
70 developed strategies to engineer them.
71
72 In this study, we redesigned the *E. coli* sigma-70 to recognize and transcribe from five orthogonal promoters
73 that are transcriptionally inactive to wild-type sigma-70, using computation-guided design and pooled cell-
74 based screens. We used Rosetta to create a customized library of computationally redesigned variants of
75 the domain of *E. coli* sigma-70 that interacts with each promoter target. Fluorescence-activated cell sorting
76 followed by deep sequencing of the sigma libraries revealed the sequence determinants of promoter
77 specificity and how they changed for different targets. We found that recognition of new promoters occurs
78 through a combination of highly conserved residues that likely make polar interactions with DNA backbone
79 and target specific adaptations. We identified orthogonal sigma variants for each of the five targets whose
80 activities ranged from 17-77% of wildtype sigma-70 on a highly active canonical *E. coli* promoter. Our
81 workflow is generalizable and can be applied to alternative sigma factors in *E. coli* and sigma factors from
82 other host organisms. The redesigned sigma factor-promoter pairs constitute an important tool for
83 engineering orthogonal genetic regulation at the genome level.
84
85 **RESULTS**
86 **The partitioned functional domains of sigma-70 enable targeted redesign of promoter specificity**
87 As the "housekeeping" regulator of transcription in *E. coli*, sigma-70 performs three functions. First, sigma-
88 70 must recognize the consensus -10 (TATAAT) and -35 (TTGACA) promoter elements. The -10 element
89 is recognized by conserved domains 2 and 3, and the -35 element is recognized by the helix-turn-helix motif
90 of domain 4 (domain 1 is unstructured) (**Fig. 1a**).[38,39] Second, sigma-70 is responsible for recruiting the
91 core RNA polymerase complex to the promoter. The interface between RNA polymerase and sigma-70 is

92 extensive (>8000 Å^2) as it spans the entire length of domains 2-4.[40] The third function of sigma-70 is to
93 mediate the melting of DNA near the -10 region, which is a critical step for initiating transcription. To operate
94 as a global regulator of cellular transcription, sigma-70 must perform each of these functions with high
95 efficiency and fidelity.
96
97 To engineer orthogonal sigma variants, we must alter promoter specificity while preserving interactions with
98 the core RNA polymerase complex and those required for DNA melting. Therefore, we aimed to restrict the
99 design to key residues of the helix-turn-helix motif of domain 4 to alter promoter specificity through the -35
100 DNA element. These include residues R584, E585, R586, R588, and Q589 (**Fig. 1a, box**). In the structure
101 of the *E. coli* transcription initiation complex (PDB ID: 4YLN), the positively charged R586 and R588 form
102 polar interactions with the negatively charged phosphate backbone to likely promote general DNA affinity.[39]
103 Specific interactions with the nucleotide bases are formed between R584:Gua-31* and E585:Ade-34* in
104 the major groove of the -35 element. Although oriented towards the major groove, Q589 does not directly
105 interact with the -35 element. Instead, Q589 is sterically packed between residues E585, R586 and R588
106 and, likely plays a role in properly orienting these critical residues within the recognition helix. Given their
107 structural roles, we hypothesized that redesigning these five key positions could engineer orthogonal
108 promoter specificity of sigma-70.
109
110 Our design workflow begins with identifying -35 element mutants that are not recognized by wildtype sigma-
111 70. These mutants became recognition targets for the computational redesign of the major groove helix
112 residues of wildtype sigma-70 (**Fig. 1b**). The top 1000 ranked designs were synthesized as chip-based
113 oligonucleotide library and evaluated in pooled fashion using a cell-based GFP screen. In this assay, high
114 GFP fluorescence signifies a specificity switch of sigma-70, as the variant must recognize the orthogonal -
115 35 element to initiate transcription of GFP. To identify specificity switches from the pooled screen, we
116 compared the distribution of variants between sorted and presorted states by deep sequencing (**Fig. 1c**).
117 Clonal screens were then used to validate several successful redesigns for each targeted -35 element.
118

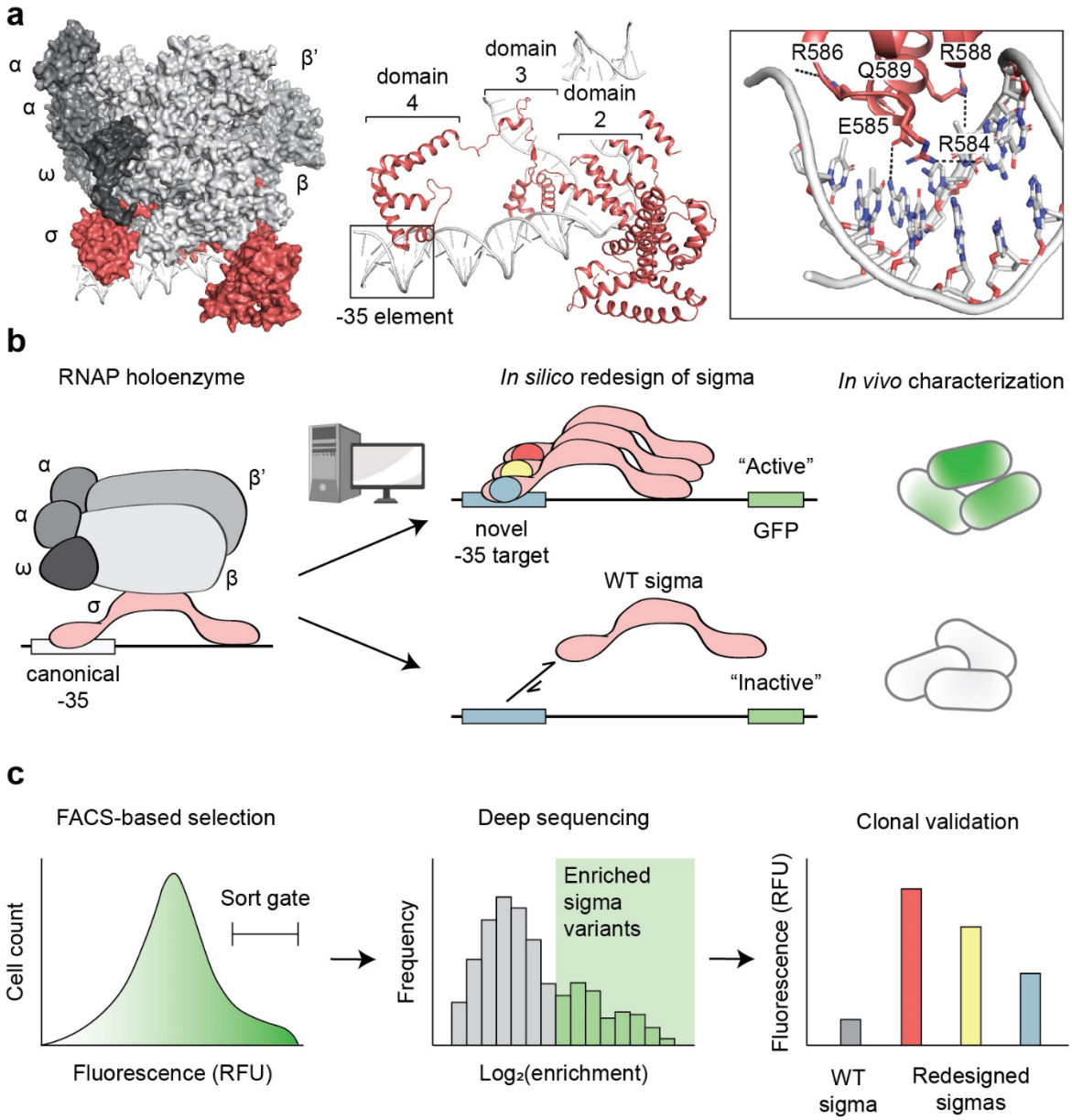

Fig. 1. Engineering sigma-70 variants with novel promoter specificity. (**a**), Structure of the *E. coli* transcription initiation complex (PDB ID: 4YLN). sigma-70 (red) bound to the -10 and -35 DNA elements (gray, cartoon representation) and RNAP core complex (gray, surface representation), composed of α (two copies), β, β', and ω subunits (left). Canonical -35 element recognized by the helix-turn-helix motif of sigma-70 domain 4 and -10 element recognized by domains 2 and 3 (middle). Orientation and h-bond contacts of residues R584, E585, R586, R588, and Q589 of the domain 4 recognition helix in the -35 major groove (right). (**b**), Workflow for altering sigma-70 promoter specificity *in silico* and characterizing function *in vivo*. Cartoon schematic of the RNAP holoenzyme with WT sigma-70 bound to the canonical -35 element (left). Replacement of the canonical -35 with a novel target and computational redesign of the domain 4 recognition helix to engineer sigma-70 variants with orthogonal promoter specificities (middle). *In vivo* functional characterization using a GFP gene placed downstream of the promoter variants containing novel -35 targets (right). (**c**), Platform for high-throughput selection and characterization of redesigned sigma-70 variants. FACS to isolate GFP positive (i.e., functional variants) (left), deep sequencing to identify enriched variants (middle), and clonal testing of redesigned sigma-70s to validate function (right).

134

135 **Synthetic promoter modifications enhance sigma-70 dependence on the -35 element**

136 As mentioned above, sigma-70 utilizes a two target DNA recognition system, with domain 4 recognizing
137 the canonical -35 element, and domains 2 and 3 recognizing the canonical -10 element. Due to this two-
138 target dependence, engineering an orthogonal sigma factor would require the redesign of multiple sigma-
139 70 DNA binding domains and their respective consensus DNA sequences. However, by artificially
140 increasing dependence of DNA recognition on the -35 DNA element, redesign is simplified to a one domain-
141 one target problem. There are several advantages to engineering orthogonality through the -35 element
142 rather than the -10 element: (1) -35 recognition is mediated by a single domain of sigma-70, (2) interactions
143 between the helix-turn-helix motif of domain 4 with the -35 major groove are structurally well understood,
144 and (3) interactions between sigma-70 and the -10 element are much more complex as transcription
145 initiation is mediated by DNA melting near this region. Thus, we sought to increase sigma-70's dependence
146 on the -35 element, and then engineer sigma-70 variants that recognize orthogonal -35 targets.

147

148 We first placed a gene encoding GFP downstream of a strong constitutive *E. coli* promoter with canonical
149 -35 'TTGACA' and -10 'TATAAT' sequences (apFab71)[41] on a "reporter plasmid" to use fluorescence as a
150 measure of transcriptional activity. As expected, a negative control lacking both canonical -10 and -35
151 promoter elements resulted in very low fluorescence relative to the apFab71 promoter (**Fig. 1a**). We
152 generated a randomized (NNNNNN) library of the -35 sequence to assess the dependence on the -10 site.
153 Moderate fluorescence was observed in the population of cells expressing the randomized -35 library,
154 suggesting that the canonical -10 element alone is partially sufficient to recruit sigma-70. To attenuate the
155 -10 dependence and increase the -35 dependence, we aimed to identify a promoter variant with high
156 transcriptional activity with the canonical -35 sequence, but significantly lower activity when paired with a
157 disrupted -10 sequence. To this end, we characterized a small subset of nucleotide deletion variants (Δ(-
158 11), Δ(-16,-7), Δ(-8), Δ(-7)) near the -10 region of apFab71. The Δ denotes deletion of a nucleotide at a
159 specific site within the -10 site. We quantified the -35 dependence of each -10 deletion variant by comparing
160 the fluorescence ratio of the deletion variant with a clonal canonical -35 and the randomized -35 population.
161 As desired, all four apFab71 promoter variants retained -35 dependence (i.e., lower fluorescence in the

162 randomized condition) and displayed approximately a 10-fold reduction in fluorescence relative to the native
163 apFab71 promoter with a randomized -35 sequence (**Fig. 2a**). The Δ(-7) promoter exhibited the greatest -
164 35 dependence with a 330-fold difference in fluorescence between the canonical and randomized -35
165 sequences. Thus, the Δ(-7) promoter was selected as the starting construct for redesigning the promoter
166 specificity of sigma-70.
167
168 **Endogenous *E. coli* sigma-70 displays very weak activity on selected -35 targets**
169 We next sought to identify a set of five promoter targets orthogonal to the canonical -35 element recognized
170 by endogenous *E. coli* sigma-70. From the library of randomized -35 sequences of the apFab71 Δ(-7)
171 promoter, we used a high-throughput 96-well screening approach to isolate and characterize promoter
172 variants not recognized by native sigma-70. We isolated 74 unique -35 variants with a 500-fold weaker
173 sigma-70 transcriptional activity (GFP fluorescence $<10^3$ RFU) relative to apFab71 (**Supplementary Table**
174 **1**). Comparing the sequences of these low activity -35 variants did not reveal a strong pattern suggesting
175 that there are many unique ways to disrupt sigma-70 promoter recognition (**Fig. 2c**). Weak conservation
176 was observed at Cyt-31 of the canonical -35 (TTGACA), but other positions deviated from the canonical
177 sequence which is also reflected by their median Hamming distance of 5 (**Supplementary Table 1**). From
178 these low activity -35 variants, we selected five diverse target sequences for engineering sigma-70 variants
179 with novel specificities: TTCATC, GGAACC, CCGCCG, GCTACC, and CCCCTC. These promoter targets
180 all displayed low transcriptional activity (500- to 900-fold lower fluorescence than apFab71), comparable to
181 the no promoter control, and vary in their composition and Hamming distances from the canonical -35
182 sequence (**Fig. 2d**). Due to their diversity, we hypothesized that these five -35 sequences present would
183 present unique design challenges and demonstrate the breadth of our redesign capabilities.
184

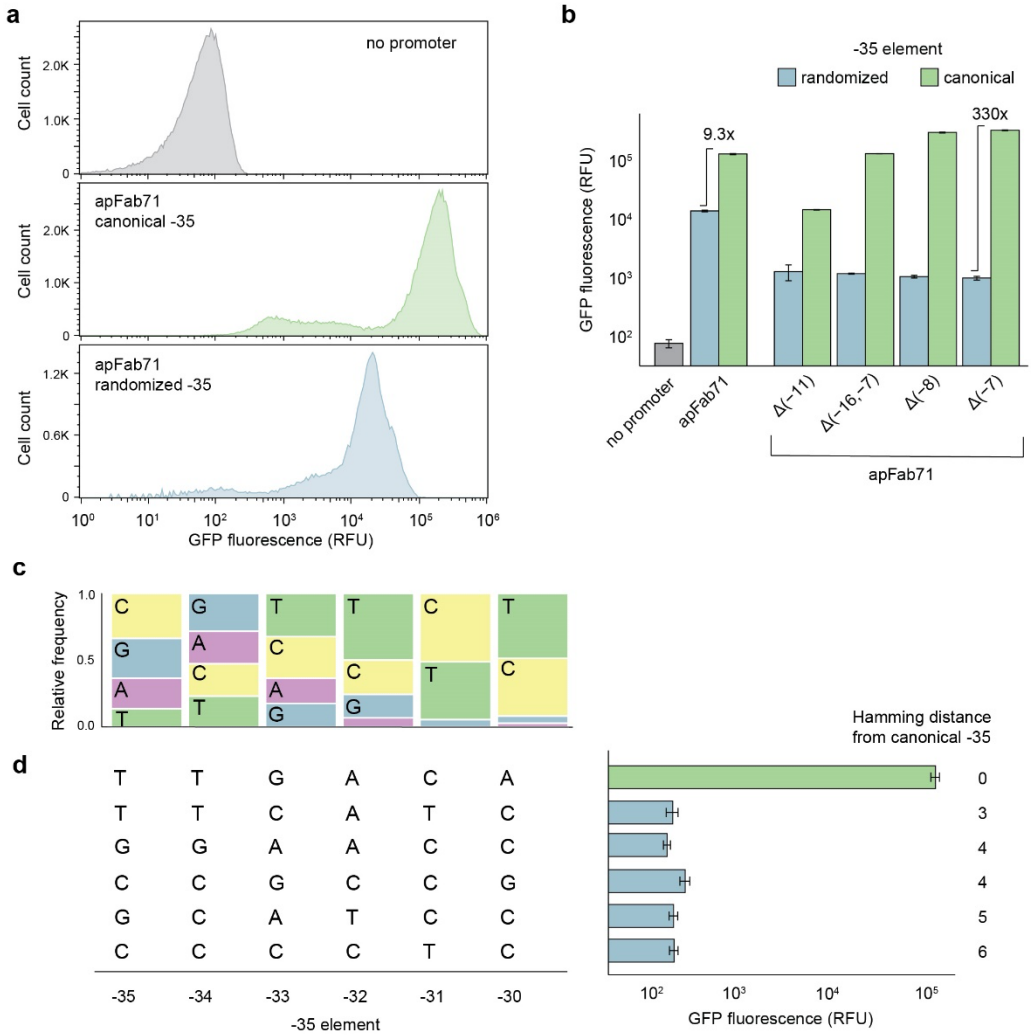

Fig. 2. Sigma-70 dependence on the -35 element and selection of orthogonal promoter targets. (**a**), Fluorescence distributions of *E. coli* cells expressing native sigma-70 and containing plasmid constructs with a GFP gene placed downstream of no promoter (gray), the strong constitutive apFab71 promoter (green), or the apFab71 promoter with a randomized -35 element (blue). (**b**), Median flow cytometry measured fluorescence of promoter variants containing nucleotide deletions (Δ) near the -10 region, and either a canonical or randomized -35 element. Fold-change between canonical and randomized -35 states was used to evaluate -35 transcriptional dependence. (**c**), Sequence logos (-35 region) of 74 unique clonal isolates with low GFP fluorescence (<10^3 RFU) (**Supplementary Table 1**). Clones were screened in 96-well format from the apFab71 Δ(-7) randomized -35 library. (**d**), Selected -35 DNA targets for engineering orthogonal sigma-70 variants. Nucleotide sequences (left) and median fluorescence (right) using native sigma-70. Error bars denote the standard deviation of replicate flow cytometry experiments (n≥2). RFU, relative fluorescence units. OD, optical density measured at 600nm.

Rosetta calculations reveal the sigma-70 sequence preferences for each promoter target

To engineer sigma-70 variants that recognize each of the five -35 targets (TTCATC, GGAACC, CCGCCG, GCTACC, and CCCCTC), we first performed large-scale combinatorial mutagenesis of residues R584,

202 E585, R586, R588, and Q589 in the helix-turn-helix (HTH) motif of domain 4 using the Rosetta
203 macromolecular modeling suite.[42-44] We excluded I587 because it is located along the interface of the HTH
204 and makes no DNA contacts. The design workflow is as follows. We replace the canonical -35 sequence
205 (TTGACA) of the sigma-70:DNA co-crystal structure (PDB: 4YLN, **Fig. 1a**) with a target -35 sequence that
206 we experimentally validated was unable to initiate transcription using native sigma-70 (**Fig. 1b**). Then, we
207 perform an *in silico* scan to evaluate the stability of the protein-DNA complex for all possible single, double,
208 triple, and quadruple variants (total ~724,000 sigma-70 variants) of the sigma-70 recognition helix (Fig. 1a,
209 boxed, middle panel). Calculations for all ~724,000 sigma-70 variants against the five target -35 elements
210 were performed on a high-throughput computing (HTC) system, requiring approximately 400,000
211 computing hours (2-3 weeks real-time). Computed protein:DNA interface scores for the ~724,000 sigma
212 variants in complex with the promoter targets were used to curate designs for experimental testing (**Fig.
213 3a, Supplementary Fig. 1a**). Lower interface scores indicate a more stable complex. Interestingly,
214 differences between median interface scores among sigma-70 variants revealed a hierarchy of promoter
215 preference of the sigma-70 scaffold (TTGACA < TTCATC < GGAACC < CCGCCG < GCATCC < CCCCTC)
216 with interface scores decreasing with increasing Hamming distance from the consensus -35 sequence,
217 TTGACA.
218
219 This suggests a smooth binding landscape of sigma-70 DNA recognition where incremental mutations from
220 the canonical -35 sequence decrease binding strength. To assess sigma-70 sequence preferences with
221 each promoter, we computed position-specific amino acid enrichment scores (E_{score}) for the top 1000
222 scoring interfaces (**Fig. 3b, Supplementary Fig. 1b**). We observed that substitutions at positions 584 and
223 589 did not have an impact on the protein-DNA interface scores suggesting that these are indirect contacts
224 that likely do not drive affinity. Nonetheless, the most enriched residue at both positions was not the wildtype
225 amino acid and was distinct for each promoter site. This suggests that though these may be indirect
226 contacts, they could play a role in promoter specificity. In contrast, positions 585, 586 and 588 show subtle,
227 but distinct preferences for different binding sites. Enrichment heat maps indicate sigma-70 positions 585,
228 586, and 588 undergo stringent selection across all -35 targets. These positions directly contact DNA in the
229 crystal structure of native sigma-70 in complex with the canonical (TTGACA) -35 element (**Fig.1a**). As

230 expected, positively charged and/or large hydrophobic amino acids are generally preferred at these
231 positions, which can facilitate highly favorable hydrogen bonding, electrostatic and/or van der Waals
232 interactions with the DNA. For all promoters, arginine and tyrosine were the most enriched amino acids at
233 positions 586 and 588, respectively. Both residues make non-specific hydrogen bonds with the sugar-
234 phosphate backbone of DNA (**Fig. 3c, Supplementary Fig. 1c**). Clear differences in amino acid preference
235 were evident for position 585. For the -35 target TTCATC, arginine was the most enriched amino acid,
236 which forms two hydrogen bonds with Gua-35* in the Rosetta structural models. Similarly, a single hydrogen
237 bond is formed by tryptophan at position 585 with Gua-35* or Thy-35* for promoters CCCCTC and
238 GCATCC, respectively. In contrast, bulky hydrophobic residues phenylalanine and leucine make van der
239 Waals contacts with the CCGCCG and GGAACC promoters. Because positions 584 and 589 do not directly
240 interact DNA, substitutions at these positions had less distinct effects on the Rosetta computed interface
241 scores.
242
243 The redesigned sigma-70 variants were ranked by binding energy, and the highest affinity 1000 variants
244 for each target -35 element were selected for experimental testing. In addition, for targets TTCATC,
245 GGAACC, and CCGCCG, we selected 1000 variants with binding energies comparable to native sigma-70
246 and the canonical -35 element (-26.0 REU), as this affinity may be optimal for DNA recognition and promoter
247 release during transcription initiation. For GCATCC and CCCCTC, the “highest affinity” and “WT-like” sets
248 were identical because the binding energy distributions of these targets were less favorable (**Fig. 3a**). We
249 synthesized these variant libraries on an IPTG-inducible plasmid expression system using oligonucleotide
250 chip synthesis and one-pot cloning.
251

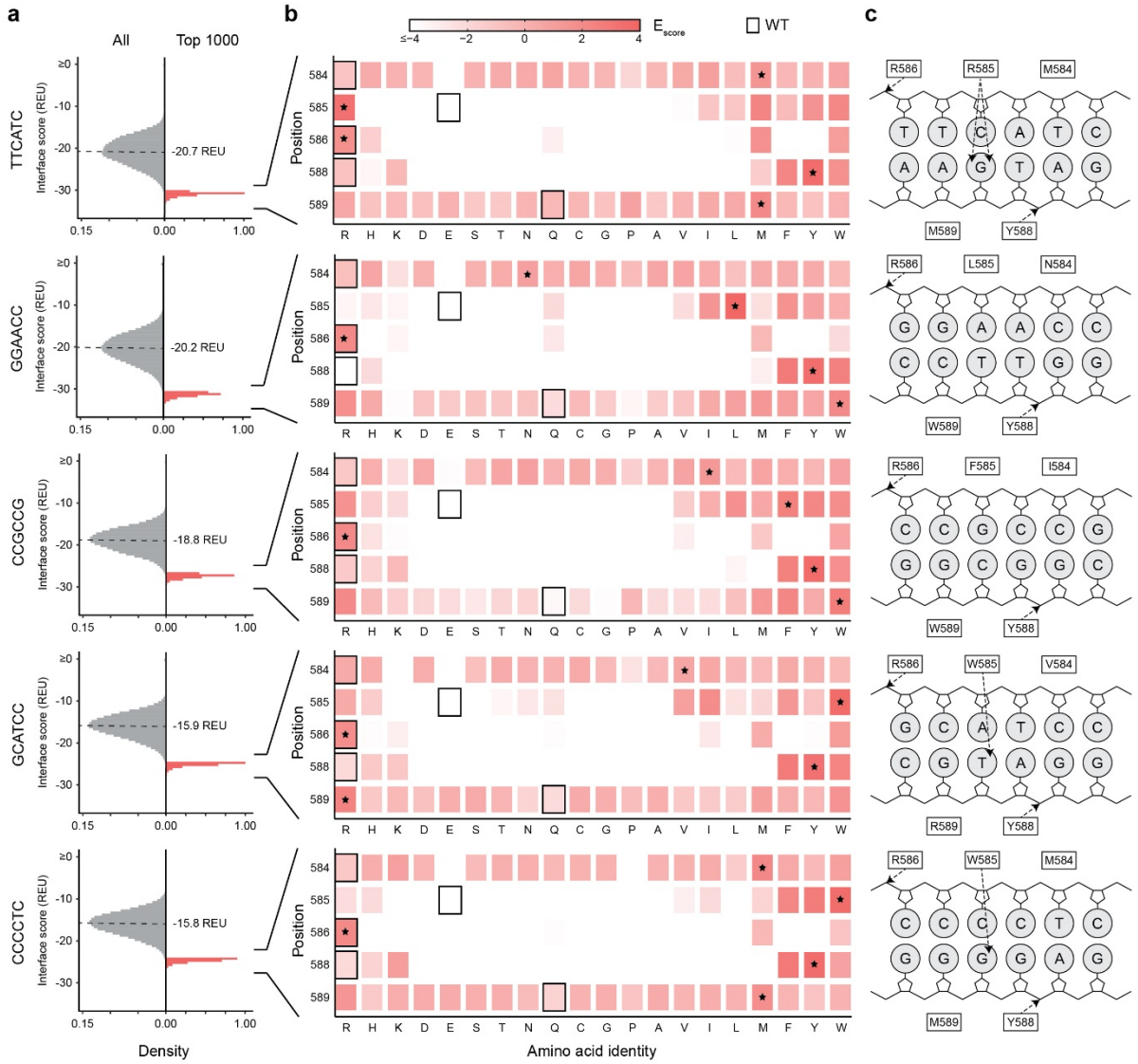

Fig. 3. Rosetta guided design of sigma-70 variants for each promoter target. (**a**), Interface scores of all (gray) or 1000 top scoring (red) sigma-70 variants in complex with each -35 DNA target. Dashed lines indicate the median interface scores of all single, double, triple, and quadruple combinatorial variants of sigma-70 positions 584, 585, 586, 588, and 589 modeled with Rosetta. (**b**), Position-specific amino acid enrichment scores (red gradient) among selected top scoring sigma-70 variants. WT identity (boxed outline) and most enriched amino acid (*) at each mutable position. (**c**), Cartoon schematic showing H-bonds formed between each enriched sigma-70 consensus sequence and -35 DNA target in the Rosetta structural models.

Isolation and identification of sigma-70 variants with novel promoter specificities

To synthesize the computationally curated library of sigma-70 designs for each promoter target, we used chip-based oligonucleotides and one-pot cloning. The library of sigma-70 designs for each target was independently cloned into an expression plasmid and placed under IPTG control. Each library was

266 transformed into *E. coli* harboring their cognate reporter plasmid i.e., GFP gene placed downstream of the
267 respective target -35 element. Due to the "housekeeping" role of sigma-70, overexpression of a sigma-70
268 variant can competitively sequester the RNAP core enzyme to inhibit cell viability. This toxicity challenge
269 has been reported in previous works using heterologous sigmas and domain swaps.[33-35] To identify an
270 expression level with minimal toxicity, we first varied the IPTG inducer concentration in a clonal growth
271 assay. Minimal growth deficiency was observed using 5μM IPTG, and thus, this concentration was used
272 for all subsequent experiments (**Supplementary Fig. 2**).
273
274 To isolate and enrich high activity sigma-70 redesigns, we sorted the high fluorescence subpopulation of
275 each library in the IPTG induced condition. Comparison of the fluorescence distributions of cell populations
276 in the induced and uninduced states show distinctly higher fluorescence in the induced condition for all five
277 target promoters (**Fig. 4a, Supplementary Figs. 3,4a**). This suggested that some sigma-70 redesigns may
278 indeed be able to successfully transcribe from an orthogonal -35 sequence. The presorted and sorted
279 libraries were deep sequenced to identify sigma-70 redesigns that were enriched after selection.
280 Approximately 10-15% of all sigma-70 variants within each 1000-member library were enriched (**Fig. 4b,**
281 **Supplementary Fig. 4b**). Taken together, these results validate our *in silico* redesign approach and high-
282 throughput screening platform.
283
284 **Sequence profiles of redesigned sigma-70 variants are unique to each -35 target**
285 Following deep sequencing, we evaluated the sigma-70 sequence profiles among enriched library variants
286 of each -35 target. Given that the 5 promoter targets are separated by a median Hamming distance of 4,
287 we expected the variable positions of sigma to undergo unique sequence selection (i.e., position-specific
288 amino acid enrichment) to recognize each -35 target (**Supplementary Fig. 5**). While some similarities are
289 shared across the sequence profiles for the five targets, each consensus sequence is unique (**Fig. 4c,**
290 **Supplementary Fig. 4c**). Arginine was highly enriched at position 586, whereas both tyrosine and arginine
291 were enriched at position 588 for all targets. In the WT sigma-70:DNA co-crystal structure (PDB: 4YLN)
292 and Rosetta structural models, positions 586 and 588 interact primarily with the sugar-phosphate backbone
293 of DNA (**Fig. 3c**). Thus, the enrichment of charged and/or polar residues at these positions is consistent

294 with forming favorable non-specific DNA interactions. These structures also show base-specific interactions
295 facilitated by position 585, which is where we observe several differences in enrichment across the
296 promoter targets: arginine is favored by targets TTCATC and CCGCCG, bulky hydrophobic residues (I, F,
297 and L) by GGAACC, aromatic residues (W, Y, and F) by CCCCTC and a wider range of residue types (W,
298 R, I, and F) by GCATCC (**Fig. 4c**). Selection was less stringent at positions 584 and 589 of sigma-70 for
299 all targets, as a broad range of amino acid identities were found among enriched variants. These positions
300 often do not directly interact with the promoter in the Rosetta models. However, charged residues (R and
301 H) were more enriched at positions 584 and 589 by targets GGAACC and GCATCC, which may
302 electrostatically enhance DNA affinity. Additional interactions may be required to facilitate binding because
303 the interactions by position 585 with the respective -35 targets are less specific. These results demonstrate
304 that promoter specificity of sigma-70 is dictated by compounding differences in primary sequence that
305 modulate both base-specific and general DNA affinity interactions.
306

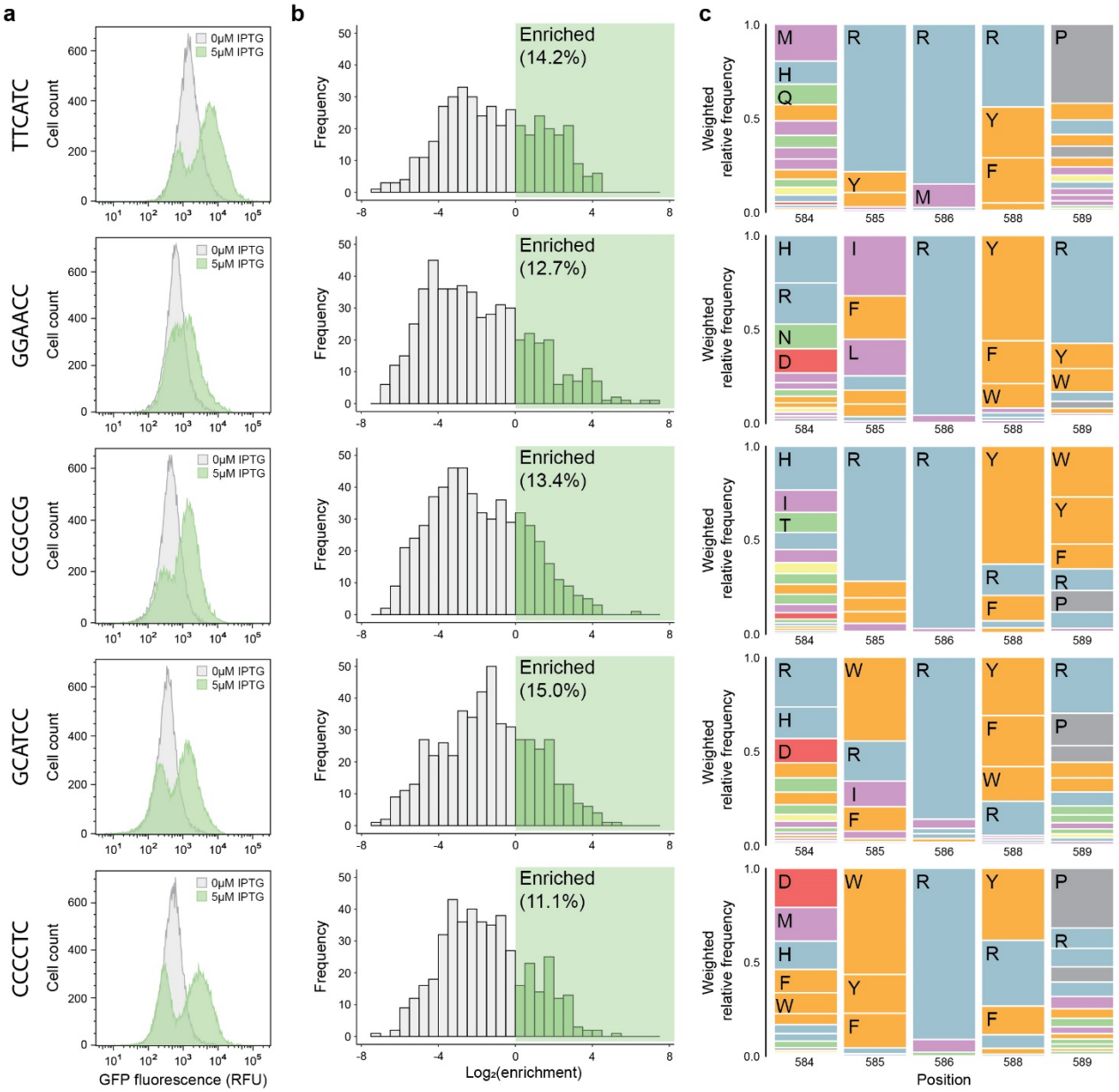

Fig. 4. Selection and identification of successfully redesigned sigma-70 variants. (**a**), Flow cytometry fluorescence distributions of uninduced (gray) and IPTG induced (green) sigma-70 variant populations for each -35 target after FACS-based selection of functional redesigns. Transcriptionally active variants were enriched using two rounds of sequential GFP positive cell sorting. (**b**), Distributions of log-transformed enrichment scores of all characterized sigma-70 variants after selection. Deep sequencing was performed on the presorted and sorted libraries to compute enrichment ratios. (**c**), Sequence logos showing the weighted amino acid frequencies at each mutable position among functionally enriched sigma-70 variants. Amino acid identities are colored by chemical properties: polar amino acids (N, Q, S, T) shown in green, basic (H, K, R) blue, acidic (D, E) red, hydrophobic (A, I, L, M, V) purple, aromatic (F, W, Y) orange, and other (C, G, P) gray.

320 **Redesigned sigma-70's exhibit varying levels of activity on the promoter targets**

321 To validate the results of our high-throughput screen, we evaluated the activity of clonal isolates from our
322 redesigned sigma-70 libraries. A total of 96 clones from the sorted libraries were randomly sampled, and
323 from this set, we were able to identify redesigned sigma-70s with activity on each of the five promoter
324 targets (**Fig. 5a, Supplementary Table 2**). To assess the performance of each sigma variant, we first
325 measured the fluorescence of cells containing the target promoters upstream of GFP in the presence of
326 endogenous WT sigma-70. Under this condition, the promoter variants yielded low fluorescence (<400 RFU
327 OD^{-1}) for the TTCATC, GGAACC, CCGCCG, GCTACC, and CCCCTC targets (**Fig. 5a**). In comparison, the
328 activity of endogenous WT sigma-70 on the canonical -35 element (TTGACA) resulted in much higher
329 fluorescence (10,200 ± 800 RFU OD^{-1}) (**Supplementary Fig. 6**). Next, we measured the fluorescence of
330 each clone on their respective -35 target sequence. Of the 96 colonies screened, 25-50% exhibited activity
331 resulting in at least a four-fold increase in fluorescence over the endogenous WT sigma-70 baseline on the
332 target promoter (**Supplementary Table 2**). The proportion of 'successful' redesigns in the sorted libraries
333 is consistent with the flow cytometry profiles (**Fig. 4a**). The activities of the top three performing sigma-70
334 redesigns for each target varied across the targets. The best performing design had 77% of the activity of
335 endogenous WT sigma-70 on the canonical -35 element (**Fig. 5a**). For the target TTCATC, which is closest
336 in Hamming distance to the canonical -35 sequence (**Fig. 2d**), we found the three highest performing
337 redesigned sigma-70s (CRRVY, FIQRY, and FWCRY). However, performance does not scale with
338 Hamming distance, suggesting a more complex relationship exists between a given -35 target and the
339 success of computationally redesigned sigma-70s.

340

341 **Rosetta structural models reveal potential mechanisms of -35 target recognition**

342 In addition to the low transcriptional activation by WT sigma-70, the five -35 targets were selected due to
343 their sequence deviation (i.e. orthogonality) from the canonical -35 and each other. The utility of engineered
344 sigma factors is dependent on minimizing crosstalk between various sigma factor-target pairs. By targeting
345 diverse -35 sequences with our redesign of sigma-70, we sought to generate novel and specific protein-
346 DNA interactions for each sigma factor-target pair. Evaluating Rosetta structural models generated for the
347 highest performing sigma-70 redesigns, we observe several differences between the hydrogen bonding

348 patterns of our redesigned sigma-70 variants with their cognate -35 targets (**Fig. 5b).** Some interactions
349 were largely conserved across target sequences, such as the h-bonds between residues 586 and 588 of
350 sigma and the sugar-phosphate backbone of nucleotides -35 and -*31, despite the diverse polar and
351 charged residues employed to maintain these interactions. In contrast to the other -35 targets, the hydrogen
352 bonding patterns of the top three performing sigma-70 redesigns for targets CCGCCG and CCCCTC are
353 highly converged. The base-specific interactions between CCGCCG and variants IRRYY, HRRYY, and
354 CRRYY occur between R585:Gua-33 and Y589:Gua-34*. For CCCCTC, a single base-specific interaction,
355 W585:Gua-33*, appears sufficient for recognition by sigma-70 variants CWRRP, FWRRP, and MWMRP,
356 perhaps necessitating the additional non-specific h-bond between R586 and the sugar-phosphate
357 backbone. However, the number of h-bonds present in these protein-DNA structural models ranges from
358 one to four, which highlights the importance of other types of molecular interactions (van der Waal's, dipole-
359 dipole) for promoter recognition. Though computationally derived, these models show how unique sets of
360 interactions may facilitate -35 target recognition by our successfully redesigned sigma-70 variants.
361
362 To understand the relationship between the Rosetta interface scores and the performance of each sigma-
363 70 redesign, we compared these energies to the enrichment scores from our high-throughput screen (**Fig.**
364 **5c**). While the computational screening approach was successful at generating functional variants and
365 significantly reduced the sequence space search from 3.2 million (20^5) combinations to a manageable
366 1000-member test set, the highest affinity redesigns (i.e. lowest interface scores) were not among the best
367 performing. This underscores the necessity of our high-throughput screening platform using FACS and
368 deep sequencing to isolate functional redesigns. The top three performing sigma-70 variants for each -35
369 target had Rosetta interface scores comparable to that of WT sigma-70 on the canonical -35 element (-
370 26.0 REU), suggesting that an 'optimal binding affinity' exists for DNA recognition and transcription initiation
371 by sigma-70. An optimized affinity may facilitate proper association with the promoter and allow dissociation
372 of sigma-70 to initiate transcription and elongation.
373

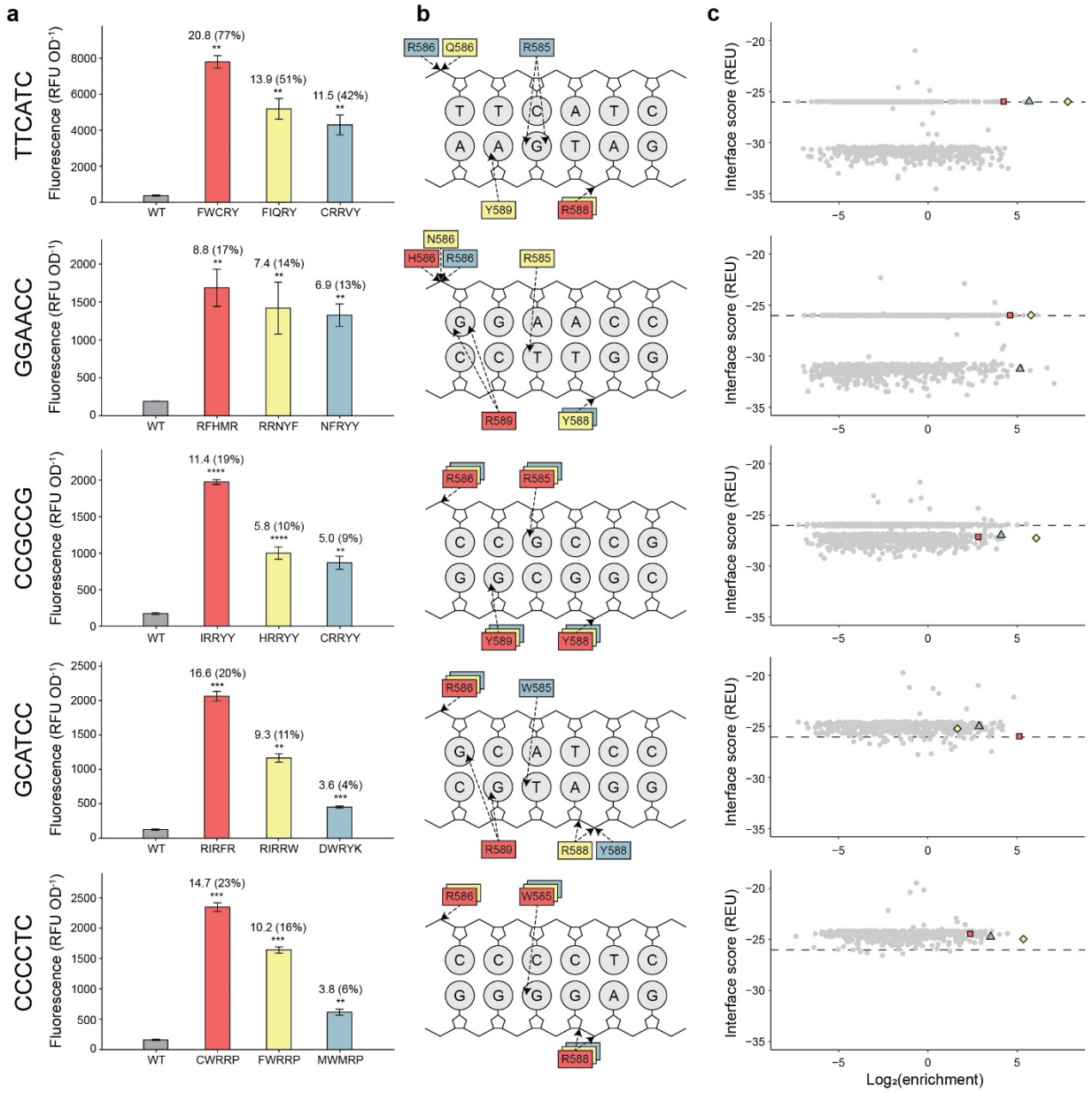

Fig. 5. Clonal validation of redesigned sigma-70 variants. (**a**), Normalized fluorescence of WT sigma-70 (gray) and the top three performing variants (red, yellow, or blue) for each promoter target. Clones were selected from the sorted libraries and assayed in a 96-well fluorescence plate reader. Error bars denote the standard deviation (**P ≤ 0.01, ***P ≤ 0.001) of replicates (n≥3) and computed fold-changes are relative to the fluorescence resulting from endogenous WT sigma-70 with each target. Percentages of activity are relative to the activity of endogenous WT sigma-70 with the promoter containing a canonical -35 element (**Supplementary Fig. 6**). RFU, relative fluorescence units. OD, optical density at 600nm. (**b**), Cartoon schematic showing H-bonds formed between each sigma-70 variant and the cognate -35 DNA target in the Rosetta structural models. (**c**), Rosetta interface scores and enrichment scores from the high-throughput screen of all tested sigma-70 variants. The top three performing variants are indicated in red (square), yellow (circle), and blue (triangle).

388 **DISCUSSION**

389 We devised a high throughput *in silico* modeling and *in vivo* screening workflow to redesign promoter
390 specificity of the *E. coli* "housekeeping" regulator of transcription, sigma-70. Using this workflow, we
391 identified multiple sigma-70 variants that activate transcription on 5 target promoters containing diverse -
392 35 elements: TTCATC, GGAACC, CCGCCG, GCTACC, and CCCCTC. These results demonstrate that the
393 promoter specificity of an essential primary transcription regulator can be rationally redesigned. Although
394 the process of transcription initiation (i.e. promoter recognition and DNA melting) by sigma factors is
395 complex, the partitioned functional domains of sigma factors enabled key interactions between the domain
396 4 recognition helix and the -35 DNA element to be redesigned without perturbing other functions. Our
397 success across all five target sequences demonstrates the extant at which promoter specificity can be
398 altered and the generalizability of our approach. Given that the Hamming distance separation ranges from
399 three to six (of 6 nucleotide positions) between these novel -35 elements and the canonical -35 element,
400 TTGACA, our approach also enables the design of sigma factors with maximal orthogonality from natural
401 sigma factors and thereby, greater potential to minimize crosstalk between synthetic and host expression
402 systems. In contrast, sigma factors generated in previous works using domain swaps of alternative sigma
403 factors or introduced from non-host family bacteria, have been limited in their orthogonality and host
404 compatibility.

405

406 One advantage to the engineered sigma-70 variants presented is that they integrate seamlessly into the *E.*
407 *coli* host, as they utilize the same endogenous transcriptional machinery. While the level of activation varied
408 from 3-fold to 20-fold across our top performing redesigns, we show that this activity was also engineered
409 *de novo*, as the native sigma-70 exhibited little to no activity on each of the orthogonal promoters. Using
410 structural models of these successful redesigns in complex with their cognate promoters, we observe
411 diverse combinations of interactions that facilitate promoter recognition. This diversity extends even among
412 successful redesigns for the same promoter target, demonstrating the utility of computational tools to
413 navigate the energetic landscape and simplify the sequence space to be experimentally tested.

414

The transcription-level regulatory complexity of a cell is mediated by the concerted efforts of global and local regulators. While many existing synthetic expression systems are reliant solely on local regulators (i.e. natural or synthetic transcription factors) to control a sparse set of genes, they lack the complexity and capabilities of native systems. Only by incorporating global regulatory components, such as engineered sigma factors, can we expand the utility and complexity of synthetic genetic circuits. However, building or isolating an extensive repertoire of global regulatory components is challenging because they must be (1) orthogonal to host systems to minimize crosstalk between the synthetic and native expression networks, (2) display dynamic control by activating gene expression in response to simple input signals, and (3) be highly customizable and modular, such that they can be easily integrated into established expression systems. Here, we developed and validated a generalizable approach to engineer sigma-70 variants that satisfy all these requirements and can be similarly applied to any host sigma factor to expand the set of available global regulatory components. Future work could pair these engineered sigma-70 factors with existing local regulators of transcription in a biosynthetic expression system.

ACKNOWLEDGEMENTS

This work was partly supported by the NIH Director's New Innovator's Award (DP2GM132682-01 to S.R.) and partly by the Great Lakes Bioenergy Research Center, U. S. Department of Energy, Office of Science, Office of Biological and Environmental Research (Award Number DE-SC0018409). The content is solely the responsibility of the authors and does not necessarily represent the official views of the NIH, Department of Defense, Department of Energy, or other federal agencies.

AUTHOR CONTRIBUTIONS

X.L., A.T.M., T.G., and S.R. conceptualized the project. X.L. devised the cell-based screening system, cloned the promoter library, and performed sorting and NGS experiments. A.T.M. performed the *in silico* calculations and designed the sigma variant libraries. T.G. performed clonal screens and identified the top performing sigma variants for each promoter target. X.L., A.T.M., T.G, and S.R. drafted the manuscript. A.T.M., X.L., and T.G. created the figures. S.R. supervised the work. All authors edited and approved the final manuscript.

REFERENCES

1 Ceroni, F. *et al.* Burden-driven feedback control of gene expression. *Nature Methods* **15**, 387-393 (2018). https://doi.org:10.1038/nmeth.4635

2 Gyorgy, A. *et al.* Isocost Lines Describe the Cellular Economy of Genetic Circuits. *Biophysical Journal* **109**, 639-646 (2015). https://doi.org:https://doi.org/10.1016/j.bpj.2015.06.034

3 Müller, I. E. *et al.* Gene networks that compensate for crosstalk with crosstalk. *Nature Communications* **10**, 4028 (2019). https://doi.org:10.1038/s41467-019-12021-y

4 Slusarczyk, A. L., Lin, A. & Weiss, R. Foundations for the design and implementation of synthetic genetic circuits. *Nature Reviews Genetics* **13**, 406-420 (2012). https://doi.org:10.1038/nrg3227

5 Costello, A. & Badran, A. H. Synthetic Biological Circuits within an Orthogonal Central Dogma. *Trends in Biotechnology* **39**, 59-71 (2021). https://doi.org:https://doi.org/10.1016/j.tibtech.2020.05.013

6 Browning, D. F. & Busby, S. J. W. Local and global regulation of transcription initiation in bacteria. *Nature Reviews Microbiology* **14**, 638-650 (2016). https://doi.org:10.1038/nrmicro.2016.103

7 Martínez-Antonio, A. & Collado-Vides, J. Identifying global regulators in transcriptional regulatory networks in bacteria. *Current Opinion in Microbiology* **6**, 482-489 (2003). https://doi.org:https://doi.org/10.1016/j.mib.2003.09.002

8 Ishihama, A. & Shimada, T. Hierarchy of transcription factor network in Escherichia coli K-12: H-NS-mediated silencing and Anti-silencing by global regulators. *FEMS Microbiology Reviews* **45**, fuab032 (2021). https://doi.org:10.1093/femsre/fuab032

9 Taylor, N. D. *et al.* Engineering an allosteric transcription factor to respond to new ligands. *Nature Methods* **13**, 177-183 (2016). https://doi.org:10.1038/nmeth.3696

10 Rao, C. V. Expanding the synthetic biology toolbox: engineering orthogonal regulators of gene expression. *Current Opinion in Biotechnology* **23**, 689-694 (2012). https://doi.org:https://doi.org/10.1016/j.copbio.2011.12.015

11 Cameron, D. E., Bashor, C. J. & Collins, J. J. A brief history of synthetic biology. *Nature Reviews Microbiology* **12**, 381-390 (2014). https://doi.org:10.1038/nrmicro3239

12 Li, J.-W., Zhang, X.-Y., Wu, H. & Bai, Y.-P. Transcription Factor Engineering for High-Throughput Strain Evolution and Organic Acid Bioproduction: A Review. *Frontiers in Bioengineering and Biotechnology* **8** (2020).

13 Feklístov, A., Sharon, B. D., Darst, S. A. & Gross, C. A. Bacterial Sigma Factors: A Historical, Structural, and Genomic Perspective. *Annual Review of Microbiology* **68**, 357-376 (2014). https://doi.org:10.1146/annurev-micro-092412-155737

14 Lu, T. K., Khalil, A. S. & Collins, J. J. Next-generation synthetic gene networks. *Nature Biotechnology* **27**, 1139-1150 (2009). https://doi.org:10.1038/nbt.1591

15 Bervoets, I. *et al.* A sigma factor toolbox for orthogonal gene expression in Escherichia coli. *Nucleic Acids Res* **46**, 2133-2144 (2018). https://doi.org:10.1093/nar/gky010

16 Gibson, D. G. *et al.* Complete Chemical Synthesis, Assembly, and Cloning of a Mycoplasma genitalium Genome. *Science* **319**, 1215-1220 (2008). https://doi.org:doi:10.1126/science.1151721

17 Richardson, S. M. *et al.* Design of a synthetic yeast genome. *Science* **355**, 1040-1044 (2017). https://doi.org:doi:10.1126/science.aaf4557

18 Browning, D. F. & Busby, S. J. W. The regulation of bacterial transcription initiation. *Nature Reviews Microbiology* **2**, 57-65 (2004). https://doi.org:10.1038/nrmicro787

19 deHaseth Pieter, L., Zupancic Margaret, L. & Record, M. T. RNA Polymerase-Promoter Interactions: the Comings and Goings of RNA Polymerase. *Journal of Bacteriology* **180**, 3019-3025 (1998). https://doi.org:10.1128/JB.180.12.3019-3025.1998

20 Feklistov, A. RNA polymerase: in search of promoters. *Annals of the New York Academy of Sciences* **1293**, 25-32 (2013). https://doi.org:https://doi.org/10.1111/nyas.12197

21 Burgess, R. R. & Travers, A. A. Escherichia coli RNA polymerase: purification, subunit structure, and factor requirements. *Fed Proc* **29**, 1164-1169 (1970).

22 A Darst, S. Bacterial RNA polymerase. *Current Opinion in Structural Biology* **11**, 155-162 (2001). https://doi.org:https://doi.org/10.1016/S0959-440X(00)00185-8

23 Helmann, J. D. & Chamberlin, M. J. STRUCTURE AND FUNCTION OF BACTERIAL SIGMA FACTORS. *Annual Review of Biochemistry* **57**, 839-872 (1988). https://doi.org:10.1146/annurev.bi.57.070188.004203

24 Paget, M. S. Bacterial Sigma Factors and Anti-Sigma Factors: Structure, Function and Distribution. *Biomolecules* **5**, 1245-1265 (2015).

25 Kazmierczak Mark, J., Wiedmann, M. & Boor Kathryn, J. Alternative Sigma Factors and Their Roles in Bacterial Virulence. *Microbiology and Molecular Biology Reviews* **69**, 527-543 (2005). https://doi.org:10.1128/MMBR.69.4.527-543.2005

26 Gruber, T. M. & Gross, C. A. Multiple Sigma Subunits and the Partitioning of Bacterial Transcription Space. *Annual Review of Microbiology* **57**, 441-466 (2003). https://doi.org:10.1146/annurev.micro.57.030502.090913

27 Lonetto, M., Gribskov, M. & Gross, C. A. The sigma 70 family: sequence conservation and evolutionary relationships. *J Bacteriol* **174**, 3843-3849 (1992). https://doi.org:10.1128/jb.174.12.3843-3849.1992

28 Marles-Wright, J. & Lewis, R. J. Stress responses of bacteria. *Current Opinion in Structural Biology* **17**, 755-760 (2007). https://doi.org:https://doi.org/10.1016/j.sbi.2007.08.004

29 Helmann, J. D. The extracytoplasmic function (ECF) sigma factors. *Adv Microb Physiol* **46**, 47-110 (2002). https://doi.org:10.1016/s0065-2911(02)46002-x

30 Maeda, H., Fujita, N. & Ishihama, A. Competition among seven Escherichia coli σ subunits: relative binding affinities to the core RNA polymerase. *Nucleic Acids Research* **28**, 3497-3503 (2000). https://doi.org:10.1093/nar/28.18.3497

31 Cowing, D. W. & Gross, C. A. Interaction of Escherichia coli RNA polymerase holoenzyme containing σ32 with heat shock promoters: DNase I footprinting and methylation protection. *Journal of Molecular Biology* **210**, 513-520 (1989). https://doi.org:https://doi.org/10.1016/0022-2836(89)90127-7

32 Koo, B. M., Rhodius, V. A., Nonaka, G., deHaseth, P. L. & Gross, C. A. Reduced capacity of alternative sigmas to melt promoters ensures stringent promoter recognition. *Genes Dev* **23**, 2426-2436 (2009). https://doi.org:10.1101/gad.1843709

33 Rhodius, V. A. *et al.* Design of orthogonal genetic switches based on a crosstalk map of σs, anti-σs, and promoters. *Mol Syst Biol* **9**, 702 (2013). https://doi.org:10.1038/msb.2013.58

34 Gaida, S. M. *et al.* Expression of heterologous sigma factors enables functional screening of metagenomic and heterologous genomic libraries. *Nature Communications* **6**, 7045 (2015). https://doi.org:10.1038/ncomms8045

35 Bervoets, I. *et al.* A sigma factor toolbox for orthogonal gene expression in Escherichia coli. *Nucleic Acids Research* **46**, 2133-2144 (2018). https://doi.org:10.1093/nar/gky010

36 Temme, K., Hill, R., Segall-Shapiro, T. H., Moser, F. & Voigt, C. A. Modular control of multiple pathways using engineered orthogonal T7 polymerases. *Nucleic Acids Res* **40**, 8773-8781 (2012). https://doi.org:10.1093/nar/gks597

37 Studier, F. W. & Moffatt, B. A. Use of bacteriophage T7 RNA polymerase to direct selective high-level expression of cloned genes. *J Mol Biol* **189**, 113-130 (1986). https://doi.org:10.1016/0022-2836(86)90385-2

38 Barne, K. A., Bown, J. A., Busby, S. J. & Minchin, S. D. Region 2.5 of the Escherichia coli RNA polymerase sigma70 subunit is responsible for the recognition of the 'extended-10'

motif at promoters. *Embo j* **16**, 4034-4040 (1997). https://doi.org:10.1093/emboj/16.13.4034

39 Zuo, Y. & Steitz, Thomas A. Crystal Structures of the Transcription Initiation Complexes with a Complete Bubble. *Molecular Cell* **58**, 534-540 (2015). https://doi.org:10.1016/j.molcel.2015.03.010

40 Paget, M. S. B. & Helmann, J. D. The σ70family of sigma factors. *Genome Biology* **4**, 203 (2003). https://doi.org:10.1186/gb-2003-4-1-203

41 Mutalik, V. K. *et al.* Precise and reliable gene expression via standard transcription and translation initiation elements. *Nature Methods* **10**, 354-360 (2013). https://doi.org:10.1038/nmeth.2404

42 Thyme, S. & Baker, D. in *Homing Endonucleases: Methods and Protocols* (ed David R. Edgell) 265-282 (Humana Press, 2014).

43 Ashworth, J. *et al.* Computational redesign of endonuclease DNA binding and cleavage specificity. *Nature* **441**, 656-659 (2006). https://doi.org:10.1038/nature04818

44 Joyce, A. P., Zhang, C., Bradley, P. & Havranek, J. J. Structure-based modeling of protein: DNA specificity. *Brief Funct Genomics* **14**, 39-49 (2015). https://doi.org:10.1093/bfgp/elu044

45 Campbell, E. A. *et al.* Structural Mechanism for Rifampicin Inhibition of Bacterial RNA Polymerase. *Cell* **104**, 901-912 (2001). https://doi.org:https://doi.org/10.1016/S0092-8674(01)00286-0

46 Murakami, K. S., Masuda, S., Campbell, E. A., Muzzin, O. & Darst, S. A. Structural Basis of Transcription Initiation: An RNA Polymerase Holoenzyme-DNA Complex. *Science* **296**, 1285-1290 (2002). https://doi.org:10.1126/science.1069595

47 Thyme, S. & Baker, D. Redesigning the specificity of protein-DNA interactions with Rosetta. *Methods Mol Biol* **1123**, 265-282 (2014). https://doi.org:10.1007/978-1-62703-968-0_17

48 Maguire, E. J., Rocca-Serra, P., Sansone, S.-A. & Chen, M. in *Eurographics Conference on Visualization.*

576 **METHODS**

577 **Rosetta design**

578 Rosetta design focused on *E. coli* sigma-70 positions R584, E585, R586, R588 and Q589 (PDB: 4YLN) as
579 previous research has demonstrated that these 5 positions interact with -35 region nucleotides through
580 hydrogen bonds.[45,46] Rosetta v3.9 was used for all calculations following existing Rosetta design protocol.[47]
581 5 promoters bearing different -35 sequences (TTCATC, GGAACC, CCGCCG, GCTACC, and CCCCTC)
582 were chosen after clonal testing, and were desirable due to their low transcription activity in vivo. To
583 generate starting structures for combinatorial protein mutagenesis, each promoter sequence was first
584 introduced in the WT sigma-70:DNA complex structure. Nucleotide substitutions were made at the
585 canonical -35 region (WT=TTGACA).

586

587 Input structures were subjected to energy minimization using Rosetta, and lowest energy structures from
588 50 minimizations were used as the input structure for the combinatorial protein mutagenesis scan at
589 positions R584, E585, R586, R588, and Q589. Standard resfiles were used to denote mutations at each
590 position for all variants containing single (95), double (3610), triple (68,590), and quadruple (651,605)
591 combinatorial mutants. Variants containing 5 mutations (2,476,099) were not tested due to the excessive
592 burden on computational resources. The structure of each protein variant in complex with all promoters
593 (including WT) were generated and the Protein-DNA binding affinity was scored. The binding energy was
594 reported as an average of 10 Rosetta minimized structures. In this minimization procedure, the amino acid
595 substitutions were first introduced followed by side chain rotomeric state optimization and protein backbone
596 design. Lastly, the Protein-DNA interface was optimized and scored using the DNA Interface Packer mover.
597 Out of these designs for each target promoter sequence, 1000 designs were selected based on two criteria.
598 The first criteria sought to contain variants with the highest binding affinity for target promoter sequence,
599 i.e. the lowest Rosetta Energy Units (REU). The second criteria sought to contain variants with a binding
600 energy for target sequence which was closest to the observed binding energy of WT sigma-70 on its native
601 target sequence.

602

603 The reason behind the first criterium is that low REU confers tighter binding to the target promoter
604 sequence, which could translate into higher transcription level. On the other hand, sigma-70 amino acid
605 composition and WT -35 sequence are likely the local minima through evolution. Although the pair's REU
606 is not the lowest among all variants, it might indicate that there is an optimal REU to allow tight enough
607 binding while permitting the release when RNAP moves downstream. The assumption is that tightest
608 binding hinders release. For some promoters, there might be overlap between two groups chosen
609 independently.
610
611 **Library cloning**
612 A promoter library was ordered via Integrated DNA Technology and amplified by hybridizing with a reverse
613 primer (hybridization protocol: 95°C for 3min, 55°C for 1min, 72°C for 1min). The product was subsequently
614 cleaned up using PCR cleanup kit (Omega Biotek) and stored in dH_2O. Backbone preparation started with
615 PCR amplification of plasmid pXL-9. For Rosetta designed sigma variants, 110-base pair (bp) single strand
616 DNA oligo pool containing Rosetta designed sigma fragments were ordered from Agilent. Oligo design
617 features unique priming regions at 5' and 3' for individual libraries complemented with BsaI recognition sites
618 and cutting sites to enable Goldengate cloning. 10ng of the oligo pool was used in the PCR reaction to
619 amplify individual libraries (PCR protocol: 95°C for 3min, 98°C for 20sec, 55°C for 15sec, 72°C for 8sec,
620 cycling from step 2 for 20 cycles, 72°C for 30sec). PCR product was subsequently cleaned up using PCR
621 cleanup kit (Omega Biotek) and stored in dH_2O. Backbone preparation started with PCR amplification of
622 plasmid SC101_LacI_WTsigma containing a WT sigma-70 driven by pLacO promoter. Amplified backbone
623 bared the corresponding BsaI binding and cutting sites, enabling scarless cloning. Backbone PCR was
624 cleaned up and subject to sequential digestion of DPN1 and BsaI_HF_V2 (New England Biolab) to remove
625 the template DNA and expose sticky overhangs. The digested backbone was further incubated with
626 Antarctic Phosphatase (New England Biolab) to remove 5' and 3' phosphates. The removal of those
627 phosphates prevents backbones from circularizing and creating false positive transformants. The
628 Goldengate reaction was done as described on New England Biolab. Briefly, 300ng of the backbone was
629 combined with 70ng of the library in a 20μL reaction. The mix was incubated at 37°C for 1hr and 65°C for

630 5min. Cooled reaction mix was dialyzed on 0.02μm filter in dH_2O for 1hr at room temperature. The dialyzed
631 sample was collected and stored at -20°C.
632
633 **Transformation of promoter and redesigned sigma-70 libraries**
634 Library transformation was conducted using electrocomponent DH10β *E. coli* (New England Biolab). 2μL
635 of the assembled library reaction mix was transformed with 25μL cells and recovered with 1mL SOC
636 medium at 37°C for 1hr. Multiple logs of dilutions were plated on appropriate antibiotic plate to measure
637 transformation efficiency. 4mL of LB and antibiotics were added to ensure proper growth selection. Cultures
638 were grown overnight before being stored in 25% glycerol at -80°C. For non-library transformations, 10ng
639 DNA was added directly to 25μL of cells and plated on agar plates containing antibiotics to confer selection.
640 Co-transformations were conducted by first growing cells containing one plasmid in LB medium with
641 appropriate antibiotics overnight. 1:50 back dilution was then done into 3mL LB without antibiotics. Cells
642 were allowed to grow until reaching an OD_{600nm} of 0.6 before being chilled on ice. Chilled cells were spun
643 down at 5000xg and thoroughly washed with ice cold dH_2O twice. The final cell pellet was suspended in
644 25μL of ice cold dH_2O. Electroporation was then repeated similarly to regular plasmid transformation.
645 Transformed cells were plated onto agar plates with appropriate antibiotics overnight at 37°C before storage
646 at 4°C.
647
648 **Induction and fluorescence measurement**
649 Multiple colonies were picked from agar plates and inoculated into 150μL LB medium in a 96-well plate
650 containing appropriate antibiotics. Cells were allowed to grow shaking (900rpm, multi-well plate shaker,
651 Southwest Scientific) at 37°C for around 3hr or until OD_{600nm} reached 0.6. Cultures were back inoculated
652 into two technical replicates of fresh LB medium with appropriate antibiotics at 1:20 dilution factor. After
653 around 3hr or upon reaching an OD_{600nm} of 0.3, IPTG (at final concentration of 5μM) was added to one of
654 the two technical replicates. Cells were incubated for 5hr before fluorescence measurement. Fluorescence
655 measurements were conducted using a multi-well platereader (HTX Biotek). Excitation and emissions
656 wavelengths of 485nm and 528nm (± 20) were used for all measurements. Measurements were normalized
657 by dividing fluorescence intensities by the OD_{600nm} before subtracting blank well fluorescence (cells carrying

658 no GFP). Fold-improvement was calculated by dividing normalized the IPTG induced fluorescence of
659 sigma-70 variants by the IPTG induced fluorescence of WT sigma-70 containing cells using the same target
660 promoter sequence. Average fold improvement was calculated from at least 3 biological replicates.
661
662 **Fluorescence activated cell sorting**
663 Around 25µl of reporter transformed libraries carrying a target promoter upstream of GFP were inoculated
664 into 3mL LB kan/spec-50 (kanamycin and spectinomycin at 50µg/mL) from glycerol stock and grown
665 overnight at 37°C in a shaking incubator. Cultures were inoculated into two separate 150µL fresh LB
666 kan/spec-50 in a 96-well plate at 1:50 dilution. Fresh cultures grew shaking at 37°C for 3hr or until reaching
667 an OD_{600nm} of 0.3. IPTG was added to a final concentration of 5µM to one technical replicate for induction.
668 After the addition of IPTG, cultures were grown for 5hr before being chilled on ice. Chilled cultures were
669 added to ice cold phosphate buffer saline (PBS) at 1:50 ratio and mixed well before being put back onto
670 the ice. Cell sorting was conducted using a Sony SH800 cell sorter (Sony Biotech) (condition: FCS
671 threshold=2500, 50% PMT on GFP, ultra-purity, round 8k events/second). Three independent replicates
672 were sorted. Briefly, cells in PBS were flowed through first to capture the distribution. Under 5µM IPTG
673 induced condition, top 10% cells were sorted out (at least 50k events). Sorted populations were flowed
674 through the sorter to capture sorting efficiency (percentage of cells fall back into the sorted gate). Sorted
675 cells with less than 80% efficiencies were sorted using the same gate again to improve the purity. Sorted
676 cells were recovered in 1mL LB medium shaking at 37°C. 100µL (1:10 dilution) of cells were plated onto
677 LB agar plates with appropriate antibiotics. The rest were growing overnight in 3ml LB with appropriate
678 antibiotics before being miniprepped into plasmid. Promoter library sorting was done by simply isolating 5%
679 of cells with lowest fluorescence.
680
681 **Variant identification using next generation sequencing (NGS)**
682 A pair of primers upstream and downstream of the mutated sigma-70 region were used to add partial
683 Illumina adaptors. Priming sites were at least 20 base pair away from the variable regions to ensure good
684 quality base calling during NGS. Amplicon size was 120 base pair. Amplicons were sequenced on
685 Amplicon-EZ Miseq service (Genewiz) with at least 50k reads for each sigma library. Sequenced libraries

686 were processed with PEAR pair-ended merger (quality threshold set to 35). Merged reads were processed
687 with custom script to identify variants. Briefly, sigma-70 variable regions were extracted and converted into
688 amino acids with corresponding frequency. Reads with frequencies of less than 5 were removed. Variant
689 frequency was normalized against total reads to get percentages. To compute individual variant's
690 enrichment, a variant's percentage under 10μM IPTG induction was divided by that of the condition without
691 IPTG. Sequence logos for variants with highest enrichment were generated using ISA-tools.[48]
692
693 **Clonal identification**
694 To identify functional sigma-70 variants, 100 colonies were sampled from the sorted populations. Highly-
695 functional (defined by its fold improvement level) colonies were measured using the above protocol for plate
696 reader measurements, and high performing colonies were subsequently identified using Sanger
697 sequencing. Unique high-performing variants were then inoculated in 3 mL kan/spec LB media and grown
698 overnight. Following overnight growth, plasmids from these variants were extracted using the protocol for
699 plasmid mini-prep. Following plasmid extraction, plasmids from these variants were re-transformed into
700 DH10β *E. coli* in order to normalize for variations in the *E. coli* genome of sorted cells that may have led to
701 false positives in GFP transcription during clonal testing. Using three biological replicates, the re-
702 transformed sigma-70 variants were measured once again using the induction protocol from initial clonal
703 screens. High-performing sigma-70 variants were measured alongside cells containing WT sigma-70 and
704 the orthogonal promoter sequences to ensure that fold-improvement scores are consistent across
705 measurements.
706

707 **SUPPLEMENTARY INFORMATION**

708 **Supplementary Table 1**. **Normalized fluorescence measurements of clones containing randomized**
709 **-35 sequences.** GFP fluorescence and OD_{600nm} measurements were collected with a 96-well plate reader.
710 Hamming distances for each sequence are relative to the canonical -35 element. The five selected low
711 activity -35 targets are highlighted in green.
712

-35 sequence	Normalized fluorescence (RFU OD^{-1})	Hamming distance from TTGACA
ATGACT	316	2
AAGCCA	426	3
TTATCC	488	3
TTCATC	320	3
TTCTCC	492	3
AGGATG	627	4
ATACCC	340	4
ATATCC	381	4
ATCTCT	420	4
CCGCCC	445	4
CCGCCG	491	4
CGGCCC	474	4
CTCGCC	426	4
CTGCTC	452	4
CTTTCT	436	4
GCGAGT	404	4
GCGCCT	548	4
GCGGCC	413	4
GGAACC	585	4
GTCGCC	439	4
TCTCCC	483	4
TTAGTG	494	4
TTCTTT	514	4
AAACCC	601	5
AAAGTA	497	5
AACGCC	475	5
AAGTGT	341	5
ACGGTT	434	5
AGACCC	376	5
AGAGCC	431	5
AGTTCC	478	5
ATTTTT	479	5
CCCTCC	416	5
CCTTCT	487	5
CGAGCC	413	5
CGCCCG	523	5
CGCGCC	396	5
CGGCTC	527	5
CGTCCT	533	5

CGTGCC	394	5
CGTTCT	489	5
CTCCTT	459	5
GACTCT	422	5
GATCCC	421	5
GATGCT	397	5
GATTCC	436	5
GCATCC	454	5
GCATCT	491	5
GCTTCT	560	5
GGCCCC	310	5
GTCTTT	510	5
GTTTTT	473	5
TACTTT	311	5
TATTTT	376	5
TGCGTT	327	5
TGCTTC	572	5
AATTTT	421	6
ACATTT	402	6
CACTTT	442	6
CATTGC	487	6
CCCCTC	554	6
CCTTTC	521	6
CCTTTT	314	6
CGCTTT	328	6
CGTCTT	509	6
CGTTTC	409	6
CGTTTT	401	6
GAATGT	316	6
GACTTT	354	6
GATCTT	457	6
GATTTT	363	6
GCCTTT	349	6
GCTTTT	400	6
GGCTTT	413	6

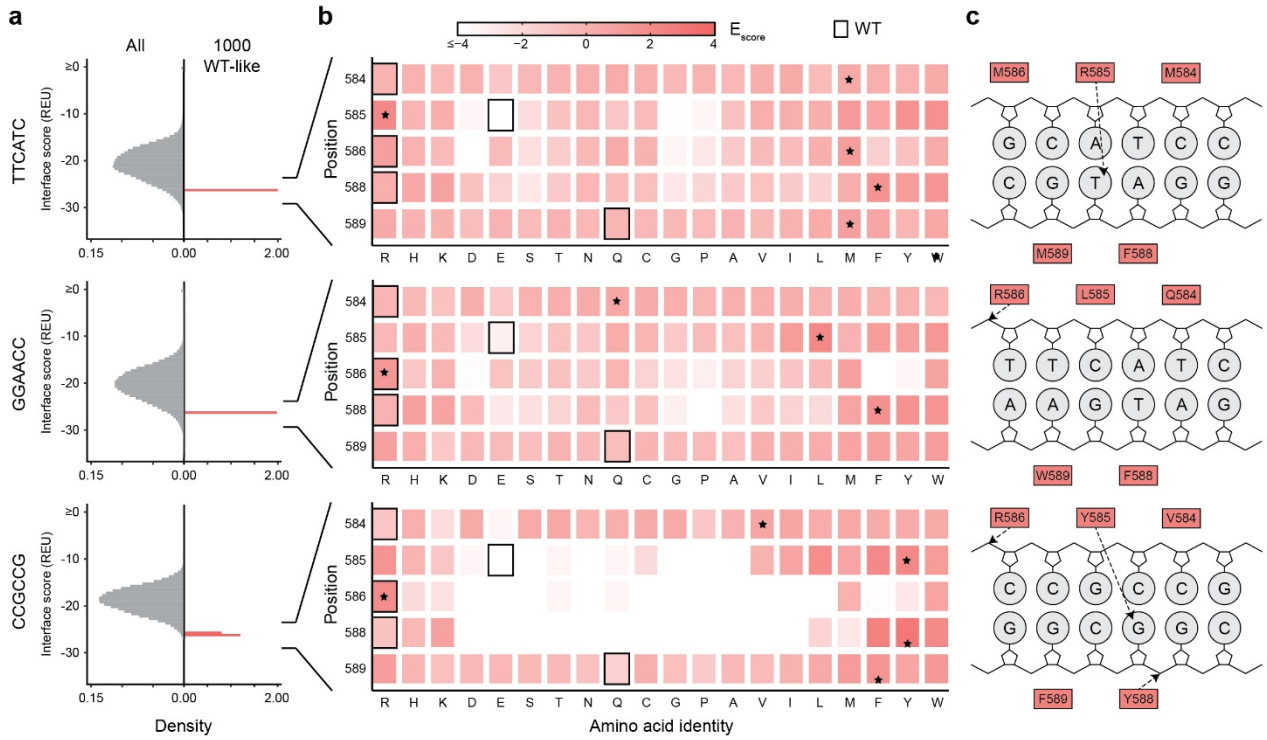

Supplementary Fig. 1. Computation-based selection of redesigned sigma-70 variants for three promoter targets. (**a**), Interface scores of all (gray) or 1000 most WT-like (Interface score = -26REU, red) sigma-70 variants in complex with each -35 DNA target. WT-like sets were not created for promoter targets CCCCTC and GCATCC because they were redundant with the lowest energy sets. All single, double, triple, and quadruple combinatorial variants of sigma-70 positions 584, 585, 586, 588, and 589 were modeled using Rosetta. (**b**), Position-specific amino acid enrichment scores (red gradient) among selected wt-like scoring sigma-70 variants. WT identity (boxed outline) and most enriched amino acid (*) at each mutable position. (**c**), Cartoon schematic showing H-bonds formed between each enriched sigma-70 consensus sequence and -35 DNA target in the Rosetta structural models.

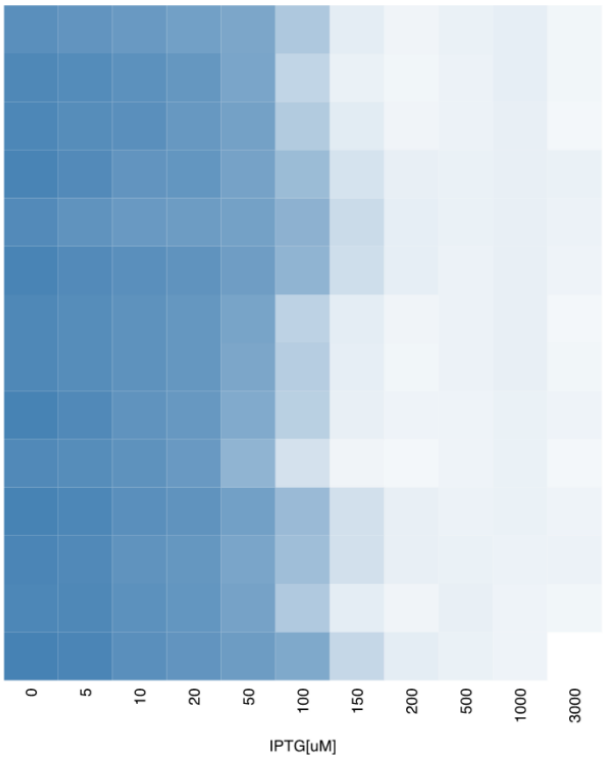

Supplementary Fig. 2. Sigma-70 expression induced toxicity. Each row corresponds to a different sigma-70 variant. Each column represents a different IPTG concentration. Color coding represents cell density measured by OD_{600}nm after 5 hours of induction. Dark represents high cell density while white represents low cell density.

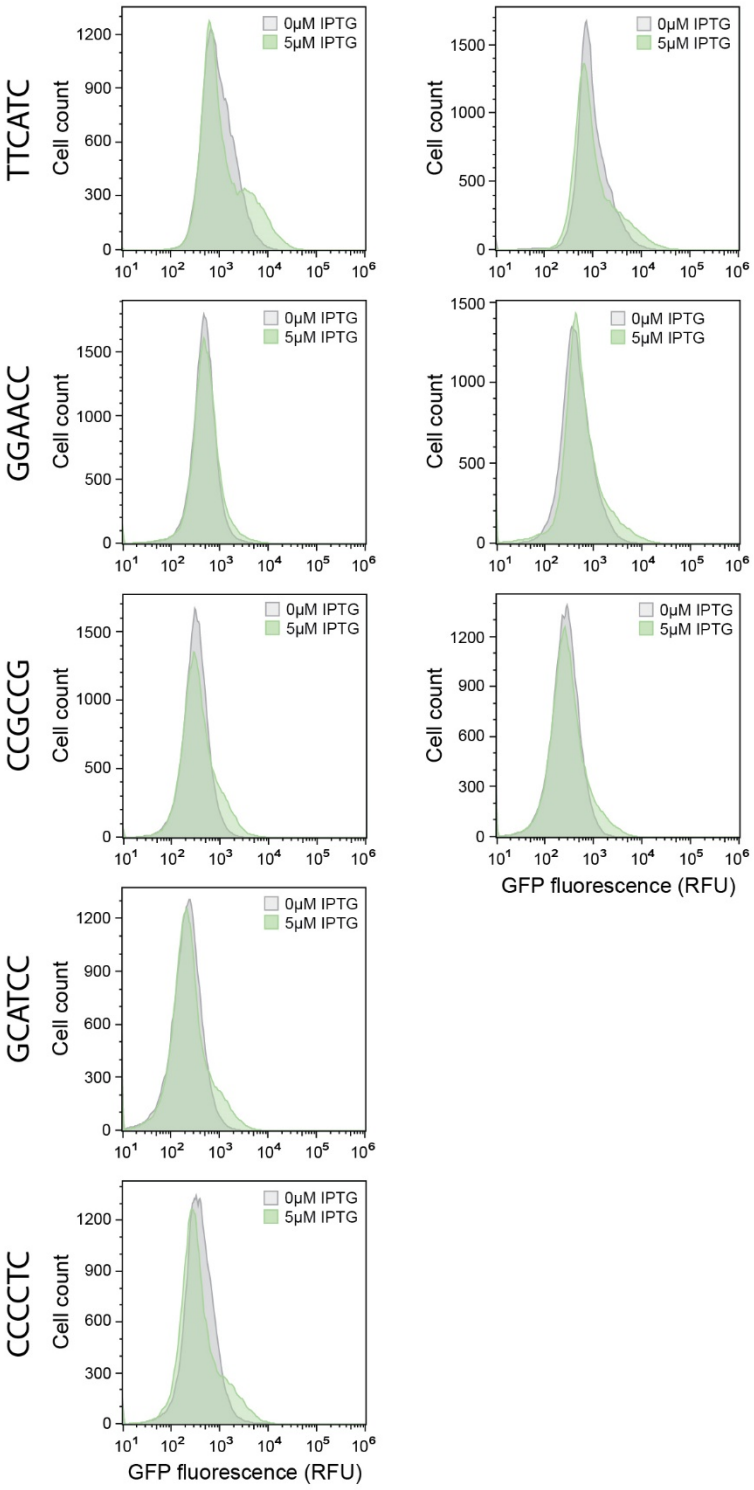

Fig. 3. Selection of successfully redesigned sigma-70 variants. Flow cytometry fluorescence distributions of uninduced (gray) and IPTG induced (green) sigma-70 variant populations for each -35 target prior to FACS-based selection of functional redesigns. Transcriptionally active variants were enriched by sorting the GFP positive subpopulation of the lowest energy (left) and WT-like (right) libraries of each target.

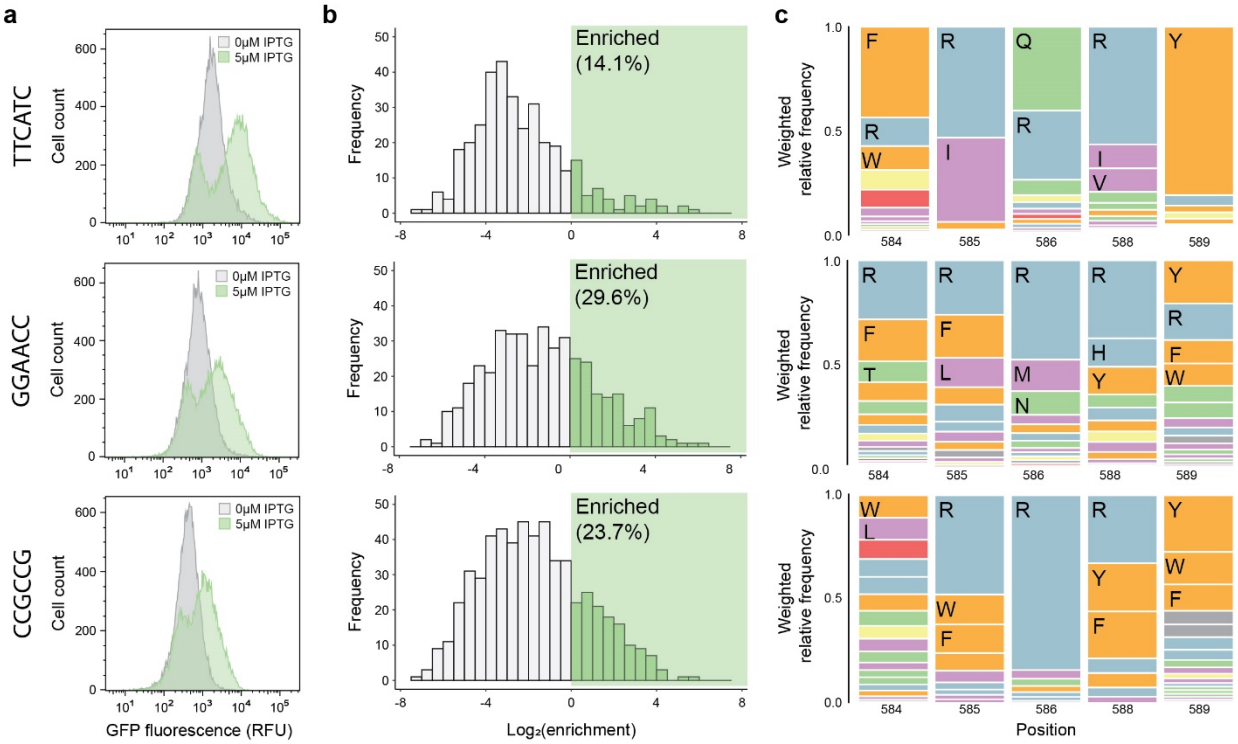

Supplementary Fig. 4. Selection and identification of successfully redesigned sigma-70 variants. (**a**), Flow cytometry fluorescence distributions of uninduced (gray) and IPTG induced (green) sigma-70 variant populations for three -35 targets after FACS-based selection of functional redesigns. Transcriptionally active variants from the WT-like libraries were enriched using two rounds of sequential GFP positive cell sorting. (**b**), Distributions of log-transformed enrichment scores of all characterized sigma-70 variants after selection. Deep sequencing was performed on the presorted and sorted libraries to compute enrichment ratios. (**c**), Sequence logos showing the weighted amino acid frequencies at each mutable position among functionally enriched sigma-70 variants. Amino acid identities are colored by chemical properties: polar amino acids (N, Q, S, T) shown in green, basic (H, K, R) blue, acidic (D, E) red, hydrophobic (A, I, L, M, V) purple, aromatic (F, W, Y) orange, and other (C, G, P) gray.

	CCCCTC	CCGCCG	GCATCC	GGAACC	TTCATC
CCCCTC					
CCGCCG	3				
GCATCC	4	4			
GGAACC	5	5	2		
TTCATC	3	6	5	4	

Supplementary Fig. 5. Hamming distances between each of the five selected -35 targets.

754 **Supplementary Table 2. Clonal screens of sigma variants after FACS-based selection of high**
755 **activity variants.** GFP fluorescence and OD_{600nm} measurements were collected with a 96-well plate reader.
756 96 clones were tested for each -35 target. Normalized GFP fluorescence was compared to WT sigma on
757 each target to compute fold-improvement.
758

-35 target	Total number of clones screened	Number of clones with fold-improvement ≥4
GGAACC	96	50
CCCCTC	96	21
TTCATC	96	51
GCATCC	96	23
CCGCCG	96	35

759
760

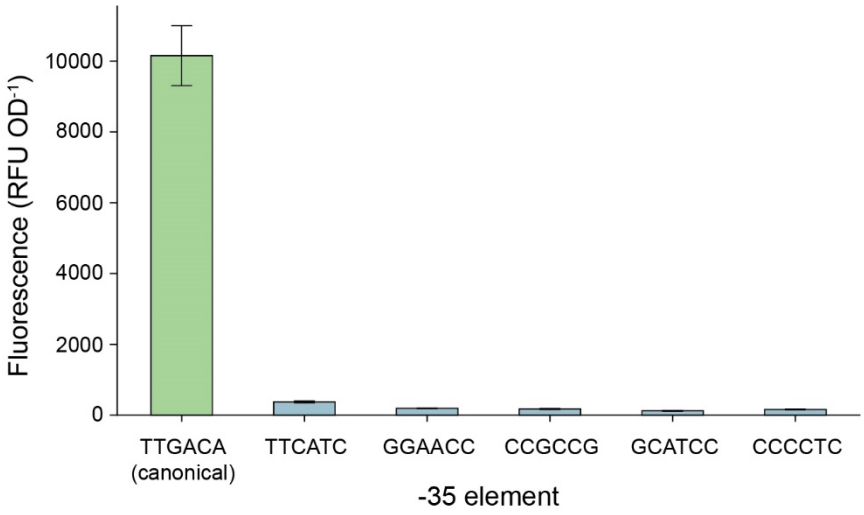

761

762 **Supplementary Fig. 6. Activity of endogenous WT sigma-70 on the canonical and target -35**

763 **elements.** GFP fluorescence and OD_{600nm} measurements ($n \geq 3$) were collected with a 96-well plate reader.